Excited-state optical transitions of excitons and biexcitons in a single In$_x$Ga$_{1-x}$As quantum disk

H. Kamada and H. Ando

NTT Basic Research Laboratories, 3-1 Morinosato Wakamiya, Atsugi, 243-01, Japan

J. Temmyo and T. Tamamura

NTT Opto-electronics Laboratories, 3-1 Morinosato Wakamiya, Atsugi, 243-01, Japan

The photoluminescence of In$_x$Ga$_{1-x}$As/Al$_x$Ga$_{1-x}$As quantum disks is investigated by microscope photoluminescence (PL) and PL excitation spectroscopies. The excited-state transitions of excitons and biexcitons are studied in terms of their dependence on excitation photon polarization. Their origins are analyzed on the basis of symmetry properties expected of excitons and biexcitons. Dominant excited-state resonances are ascribed to successive two-step absorptions of two photons of opposite optical orientation, one into an exciton excited state followed by another into a densely distributed biexciton excited state. Filling of the exciton state is found to lead to absorption from the exciton ground state to the biexciton excited state. Remaining excitation resonances with large oscillator strength are identified as two-photon absorption processes that directly create weakly correlated exciton pair states. [S0163-1829(98)05147-9]

I. INTRODUCTION

The semiconductor zero-dimensional (0D) structure has long been a subject of interest not only in physics but also in device application.[1] The activity oriented toward the realization of the semiconductor 0D structure is now approaching a new apex following the application of the spontaneous reconstruction of the strained heterostructure, such as that obtained through the coherent islanding phenomenon.[2,3] It exploits the damage-free fabrication of the quantum-dot structure. The spatial extent of such structures currently available is even smaller than the extent of twice the typical exciton Bohr radius.[3,4] In such a structure, one may observe the most distinct features of the quantum confinement effects expected for quantum dots. As the density of states between discrete levels is, in principle, zero, the scattering of electronic state which leads to dephasing of the state and follows energy relaxation may be inefficient because of the lack of final states mediating the scattering events. The inhibition of such processes may thus lead to a substantial increase in the dephasing time of the exciton states and sharp and distinct exciton resonances can be observed. The mesoscopic enhancement of exciton oscillator strength may also occur particularly when the spatial extent of the dot is greater than several times the exciton Bohr radius.[5] As a result, a very sharp exciton ground state as well as excited-state resonances are expected and these have frequently been observed in the microscope photoluminescence spectrum.[6-12]

Packing excitons into a tiny space will also enhance the interaction between two excitons with opposite spin orientations, thereby greatly increasing the biexciton effect. This has been demonstrated by Forchel *et al.*[13] for an artificially defined quantum dot, and the biexciton was observed even in a monolayer island in a GaAs/Al$_x$Ga$_{1-x}$As quantum-well interface by Brunner *et al.*[10] The lateral confinement energy in the latter case is only as low as 10 meV, nevertheless distinctive biexciton luminescence was observed, implying the potential of the 0D structure in stabilizing the biexciton state. More recently, a series of confined multiexciton lumines-

cence emissions in a self-assembled dot was reported.[14] Because the binding of biexcitons in a quantum dot is much tighter than in a three-dimensional (3D) or two-dimensional (2D) structure, biexcitons survive up to a higher temperature. Such stable biexciton is considered to be a unique consequence of the spatial confinement of quantum dots and it cannot be observed in bulk materials. As a matter of fact, the biexciton effect may dominate the optical process in quantum dots and should be seriously considered when examining the optical responses of quantum dots. Use may also be made of its specific nonlinear optical properties in device application.

Up to now, the biexciton effect has most extensively been studied in materials such as CdS and CdSe dots[15,16] which are classified as being in the ''strong-confinement'' regime. The extent of the dot in these cases is much smaller than the exciton Bohr radius. However, in the ''weak-confinement'' regime, only a few observations have been made until recently.[10,13,17] The observation of biexciton luminescence in the monolayer island in the III-V quantum well such as reported by Brunner *et al.*[10] confirmed the enhancement of the biexciton effect in grown-in monolayer islands. However, a detailed picture of the excitation of excitons and biexcitons via their discrete excited states is unclear.

In this paper, we address the optical excitation via excited states of an exciton[11,12,18] and a biexciton in a quantum dot in the weak confinement regime. We have used a unique self-organized In$_x$Ga$_{1-x}$As/Al$_x$Ga$_{1-x}$As disk structure grown on a $(311)B$ substrate.[19] The spontaneous reorganization resulted in arrays of well-ordered In$_x$Ga$_{1-x}$As disk-shaped structures with diameters of 30 to 100 nm automatically embedded in the Al$_x$Ga$_{1-x}$As.[4,20] Since the lateral extent of the relevant structure lay within a range, $R > a_B$, where R and a_B denote the lateral extent of the disk and exciton Bohr radius, respectively, exciton confinement governs the optical properties of the dot, and mesoscopic enhancement of the exciton response is still operative.[21] The quantum disk provides well-separated heavy-light valence splitting as a consequence of the larger quantum confinement perpendicular to

the quantum-well plane, thus leaving heavy-hole states as the lowest in the energy spectrum.[22–24] Additional lateral confinement leading finally to a complete quantization along all three directions gives rise to an absolutely discrete excitonic level structure, whereby sharp optical emissions and absorption[11,12,18] can be observed. To analyze the role of biexcitonic excitation in this mesoscopic dot system, we first hunt for well-correlated exciton/biexciton pairs. Due to the significant biexciton effect, an exciton is excited not only via its excited states but also via biexciton excited states. Enough large heavy and light splitting then enabled spin-selective excitation, whereby discrimination of exciton-related or biexciton-related transition was made possible via excitation of one or both spin orientations. Photoluminescence excitation (PLE) experiments on an isolated single dot were thus done with a variety of light polarizations of excitation and by detecting luminescence of particular polarization. We give a classification of the observed excitations in terms of the symmetry properties of excitons and biexcitons and recently given theoretical guidelines.[25] An important role of the weakly correlated exciton pair state with large oscillator strength is stressed.

The paper is organized as follows. In Sec. II, we present experimental details on the growth and characterization of the $In_xGa_{1-x}As$ quantum disk. In Sec. III, we first discuss the experimental results of microscope photoluminescence (PL), stressing the important biexciton effect. Results of PL excitation (PLE) measurements under a variety of polarizations and the intensity of excitation photons are given to classify the excited-state transitions into excitonic or biexcitonic origin. Then we compare the results with the expected optical selection rules and we identify the origins of some observed excited-state transitions, which we discuss with regard to recent theoretical expectations. Finally, in Sec. IV, we summarize our results.

II. EXPERIMENTAL DETAILS

The samples used for this study were all grown by low-pressure metalorganic vapor phase epitaxy on GaAs (311)B substrates, using trimethyl-gallium (TMG), trimethyl-aluminum (TMA), trimethyl-indium (TMI), and arsine as gas sources. Following the deposition of a 100-nm $Al_{0.5}Ga_{0.5}As$ buffer layer, an $In_xGa_{1-x}As$ layer with a nominal thickness of 15 nm was deposited as an initiating layer and this was subsequently capped by 150-nm-thick $Al_{0.5}Ga_{0.5}As$ [Fig. 1(a)]. A thinner $In_{0.4}Ga_{0.6}As$ disk layer with a nominal thickness of 3–6 nm was then deposited, followed by 1–3-min growth interruption to allow spontaneous disk formation[4,20] [Fig. 1(a)]. The growth temperature was between 690 °C and 750 °C. It should be noted that no $Al_xGa_{1-x}As$ overgrowth was needed to embed the $In_xGa_{1-x}As$ disk as confirmed by a secondary electron microscope image of a cleaved facet in Fig. 1(b), where we observed clear contrast between In-rich disk and Al-rich coverage. The spontaneous rearrangement resulted in $In_xGa_{1-x}As$ islanding as well as automatic $Al_xGa_{1-x}As$ coverage on top through the complex interplay of the mixing/segregation of the $In_xGa_{1-x}As/Al_xGa_{1-x}As$ heterostructure and strain minimization.[20] Due to this automatic coverage, the structure at the surface maintained good radiative efficiency without being spoiled by surface nonra-
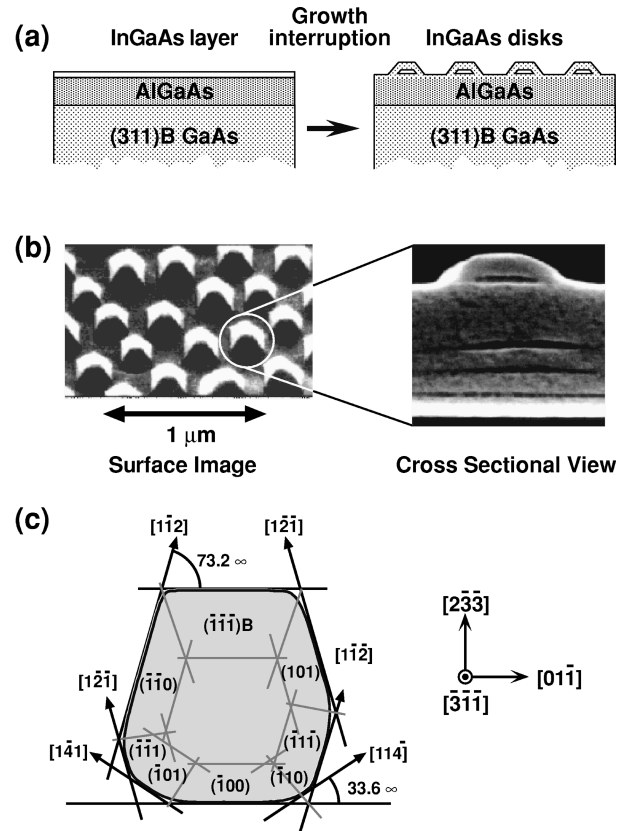
FIG. 1. Schematic representation of growth sequence to obtain an ordered array of an $In_xGa_{1-x}As$ disk: One to three minutes growth interruption results in self-organization (a). Secondary electron microscope image of the surface, left of (b), and cross-section view showing In-rich disk-part and Al-rich coverage, right of (b). Each nanocrystal in the array has a specific facet structure composed mostly of low-index surfaces as determined by atomic-force microscopy (c).

diative recombination, thereby enabling single-dot spectroscopy. Electron microscope observation confirmed the formation of an array of well-faceted nanocrystallines such as Fig. 1(b) (left) containing $In_xGa_{1-x}As/Al_xGa_{1-x}As$ disks [Fig. 1(b), right]. The disk diameter was controlled within 20 to 100 nm by a nominal indium composition, 0.2 to 0.4. 20 to 60 dots were typically found in a surface area of 2 μm×2 μm depending on the nominal indium composition of 0.2 to 0.4. Figure 1(b) is a typical secondary electron microscope image of a quantum disk sample of $In_{0.2}Ga_{0.8}As$. A well-ordered array of dot islands is evident, and each island has a peculiar facet structure composed mostly of low index surfaces such as (111), (100), and (110) as displayed in Fig. 1(c), inferring surface reconstruction into the faceted surface structure with a lower surface energy during self-organization. The symmetry is apparently low. Thus we expect that the optical properties associated with localized excitons will reflect this characteristic geometry of the dots. As we will show, this structural asymmetry can impose a lifting of the degeneracies of the dot states, resulting in a multitude of excited-state energy levels.

For single-dot luminescence spectroscopy, we used a microscope objective lens and a He-flow cryostat firmly attached on a high-precision XYZ stage.[12] The sample mounted on a cold-finger was cooled to less than 4 K. A
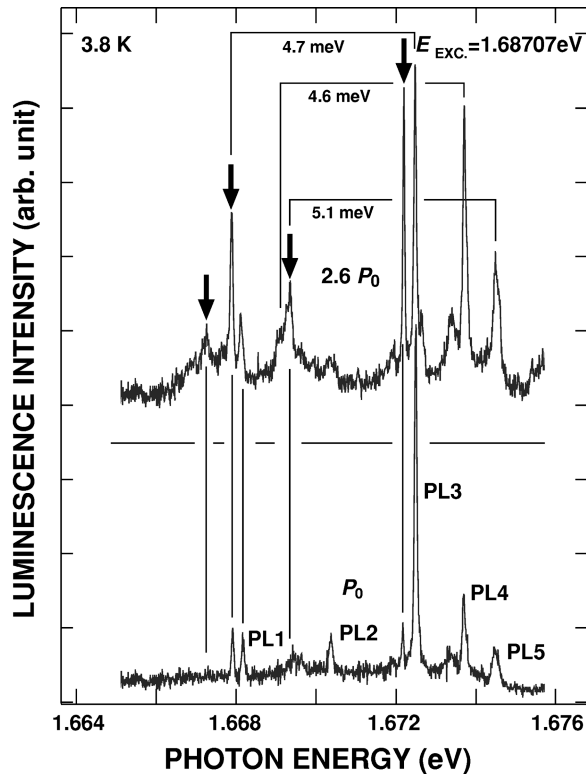
FIG. 2. Dot PL spectra taken under two different excitation densities, P_0 and $2.6\ P_0$ ($P_0 \simeq 300$ W/cm^2) at 3.8 K. Excitation energy is 1.687 07 eV. PL emissions labeled PL1 though PL5 are excitonic emissions from different dots. Arrows indicate biexcitonic PL emissions and links connect exciton and biexciton luminescence from individual dots. Biexciton binding energies are also indicated.

FIG. 3. Evolution of a series of luminescence lines under increasing excitation density (95 to 1900 W/cm^2). PL emission labeled X (PL3 of Fig. 2) is the exciton luminescence and that labeled XX is the biexciton luminescence pairing with X. Excitation energy is 1.7819 eV.

laser beam from a continuous-wave Ti/sapphire laser pumped by an Ar$^+$-ion laser was focused to a 2-μm spot on the sample surface. Luminescence was collected through the same lens, passed through a pin hole at the imaging plane which corresponded to a PL image of 2 μm in diameter, then dispersed by a 1-m double-grating monochromator. Finally it was detected by a cooled Si charge-coupled device. In order to reduce the number of dots within the laser spot and to facilitate the repeated location of specific areas on the sample, a metal mask with fine openings was processed on the sample surface. The sample was first coated with a thin dielectric film (200-nm-thick) and a thin titanium film with a variety of openings down to 0.2 μm^2 was processed by electron-beam lithography and the lift-off technique. Doing micro-PL measurements through the fine mask openings allowed only a few dots within the micrometer-sized optical probe. A well-separated small number of sharp (typical FWHM less than 200 μeV and the narrowest less than 34 μeV) luminescence lines with very high radiative efficiency were observed (e.g., Figs. 1–3).[11,12] The polarization of the laser beam was controlled by a polarizer coupled either with a half-λ or a quarter-λ plate located before the beam entrance. The former produced a linear polarized and the latter a circularly polarized excitation source. In similar ways, a linearly polarized PL component was selected by a combination of a half-λ plate and a linear polarizer, and a circularly polarized PL component was selected by a combination of a quarter-λ plate and a linear polarizer.

III. RESULTS AND DISCUSSION

A. Exciton and biexciton luminescences

We adopted the following method to identify pairs of correlated exciton and biexciton luminescences. First, by measuring the excitation power density dependence of the spectrum, we looked for the luminescence lines that grew quadratically with an increase in the excitation power. They can be attributed to biexcitonic transitions. Second, by PLE measurement on all the observed PL lines, we could correlate a particular biexciton luminescence with an exciton luminescence originating from an identical dot. Both luminescence lines may involve common resonant excitation features.[10] In the following, we present the results obtained in this way. A brief check was made as follows: The PL spectra in Fig. 2 (excitation energy 1.68707 eV) were taken on an In$_{0.4}$Ga$_{0.6}$As sample through a mask opening of 0.5 μm^2 at 3.8 K. Excitonic PL lines PL1 through PL5 are visible. By changing the excitation intensity by a factor of less than 5, from P_0 ($=300$ W/cm^2) to $2.6P_0$, the luminescence lines for biexcitonic origin (indicated by arrows) grow superlinearly by factors approximately equal to the square of the factor of the excitation intensity increase. The links in Fig. 2 represent pairs of exciton/biexciton emissions as determined by subsequent PL excitation (PLE) measurements on each lines. Nearly all the dot exciton luminescences are accompanied by biexciton partners, implying the biexciton effect is common for the present 0D structures.

From now on we will mainly focus on the properties of a single quantum dot found in the same $In_{0.4}Ga_{0.6}As$ sample. Figure 3 shows the evolution of a 4 K PL spectrum observed through the same mask opening but with a different excitation energy of 1.7819 eV for a series of excitation power densities. In general, the PL spectrum is extremely sensitive to excitation energy, reflecting a resonant excited level structure for the dot. Therefore by choosing the excitation energy, only a few dot luminescence lines can be isolated. It is noteworthy that all the excitations in this study were made resonant to excited-state resonance of the dot. Under such conditions, much higher excitation density is required to saturate dot luminescence than in the case using the excitation into the barrier continuum.[11] A range of the excitation density is required which is larger by three orders of magnitude than using Ar^+-laser excitation. Nevertheless, the dot luminescences were all very sharp and distinctive, and the linewidth was less than 100 μeV. They are ascribed to the luminescences of excitons localized in disk-shaped quantum dots.

Under an excitation density (about 3 mW per spot, corresponding to 100 W/cm^2), only the exciton line labeled X (bottom spectrum in Fig. 3) with a typical linewidth of less than 80 μeV can be observed (spectrometer resolution of 25 μeV). The additional lines visible at higher energy are from other dots within the same metal mask opening. With increasing excitation density, the intensity of the exciton luminescence nearly increases linearly, reaches maximum, and then falls very sharply for higher excitation. Simultaneously, another new distinct sharp line labeled XX emerges at an energy lower by 4.7 meV (see the spectra at 190 and 380 W/cm^2 in Fig. 3). The intensity of the latter luminescence line first increases quadratically, then it continues growing while X is fading. Such behaviors are very similar to the results reported by Brunner et al.[10] and by Forchel et al.,[13] and they are regarded as the fingerprint of a pair of exciton and biexcitonic emissions. Under a higher excitation density above 1000 W/cm^2, line broadening occurs on X as well as on XX as we previously reported.[11] Typically broadening by a factor of 2 for an excitation above 1000 W/cm^2 was observed. This is due to the ease of losing exciton coherence caused by an increasing exciton-exciton (carrier) scattering probability.

The luminescence intensity evolutions of X and XX are summarized in Fig. 4, where integrated PL intensities are plotted as a function of excitation density. The linear increase of X and the quadratic increase of XX at low excitation are quite clear.[10,13] Photon emission rates of exciton and biexciton ground states can be deduced from the occupations of those states calculated using a set of rate equations based on a simple exciton-biexciton four-level scheme (inset in Fig. 4). The equations are

$$\frac{df_0}{dt} = -Gf_0 + \frac{f_X}{\tau_r^X}, \quad (1a)$$

$$\frac{df_X}{dt} = Gf_0 - \frac{f_X}{\tau_r^X} - \alpha Gf_X + \frac{f_{XX}}{\tau_r^{XX}}, \quad (1b)$$

and
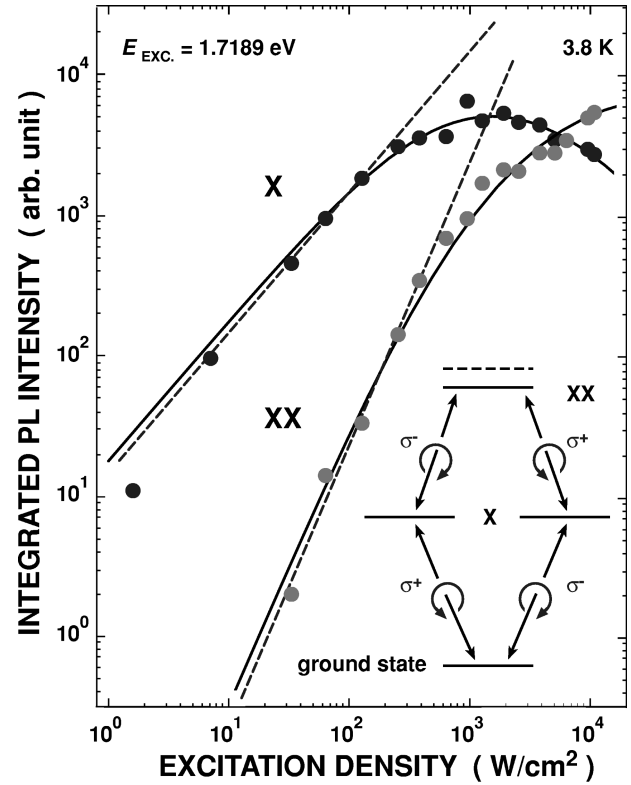
FIG. 4. Integrated luminescence intensity of an exciton and a biexciton in a single $In_xGa_{1-x}As$ quantum disk at 3.8 K plotted as a function of excitation density. Inset shows an exciton-biexciton four-level scheme with helicity-dependent transitions.

$$\frac{df_{XX}}{dt} = \alpha Gf_X - \frac{f_{XX}}{\tau_r^{XX}}, \quad (1c)$$

with $f_0 + f_X + f_{XX} = 1$, where f_0, f_X, and f_{XX}, respectively, represent the fractions of an empty dot, the exciton, and the biexciton. The parameters G, τ_r^X, τ_r^{XX}, and α are the exciton creation rate, the exciton radiative lifetime, the biexciton lifetime, and a proportional constant, respectively. The third term in Eq. (2) represents the capture of the second exciton creating a biexciton. By letting the left sides be zero and solving the resulting coupled equations, we have the fractions of the exciton and biexciton as functions of G. We estimate unknown parameters such as τ_r^X and τ_r^{XX} from our recent time-resolved PL experiment.[29] Namely, we found the exciton radiative lifetime to be 400–500 psec at 4 K. τ_r^{XX} was assumed to be of the same order. The solid lines in Fig. 4 represent the solutions to the rate equations (1a)–(1c) for excitonic PL intensities obtained by assuming $\tau_r^X/\tau_r^{XX} = 2.4$ and $\alpha = 0.2$. The value of $\tau_r^X/\tau_r^{XX} = 2.4$ may be compared with theoretical values for a mesoscopic dot: According to the calculation by Takagahara et al.,[30,31] the ratio of the biexciton oscillator strength over that of an exciton, f_{XX}/f_X, in a mesoscopic GaAs dot is about 1.8 as $R/a_B = 2$ and it is about 2 as $R/a_B = 3$. The agreement seems reasonable, although the calculation was made on a spherical dot. Therefore, the four-level exciton-biexciton model satisfactorily explains the experimental results and the exciton/biexciton attribution was reinforced.

The line X corresponds to the transition from the one-exciton ground state to the empty state, while the line XX corresponds to that from the biexciton ground state to the exciton ground state. The energies of these two transitions are in the inset of Fig. 4: the XX transition has an energy $E_{XX} - E_X = 2E_X - \Delta_{XX} - E_X = E_X - \Delta_{XX}$ $(E_{XX} = 2E_{XX} - \Delta_{XX})$, where E_X and E_{XX} denote the energies of the exciton and the biexciton, respectively, and Δ_{XX} is the biexciton binding energy. The observed PL energy separation of 4.7 meV between X and XX agrees well with the biexciton correlation energy, about 5 meV, expected for small GaAs/Al$_x$Ga$_{1-x}$As quantum-dot structures.[26] Also for the other dot luminescences in Fig. 2 we obtain biexciton binding energies of 5.14 and 4.6 meV. They are all significantly enhanced compared to the value of about 1 meV observed in QWs and that of about 0.2 meV in bulk GaAs.[27,28]

B. Exciton/biexciton energy spectra

As the disk-shaped structure provides well-separated heavy-light valence splitting as a consequence of the stronger quantum confinement perpendicular to the quantum-well plane, it leaves heavy-hole states as the lowest in the energy spectrum. Under these circumstances, spin acts like a good quantum number. Linear polarization can create both spin-up and spin-down excitons, and is thus capable of feeding not only the exciton but also creating a biexciton composed of two excitons with opposite spin orientations. A biexciton composed of two excitons with opposite spins cannot be created by circularly polarized light. Therefore the comparison of the spectra taken under linear and circular polarization may enable the distinction of the transition either of excitonic or of biexcitonic origin.

The PL excitation experiments under an excitation density (about 100 W/cm^2) on both X and XX revealed the spectra in Fig. 5. The excitation source was linearly polarized. During the recording of each spectrum, the laser power was stabilized at a constant to obtain constant excitation density PLE spectra. The PLE measurements on the number of dots revealed that the excitation spectrum was unique for each dot. It should be noted, however, that the pattern of PLE resonance structure seemed quite similar for the number of dots, differing only in level spacing and relative energies. The PLE spectrum is characterized by a number of well-separated sharp resonances, which we attribute to the exciton excited states. In two PLE spectra for X and XX, a number of sharp resonance features are common; nearly one-to-one correspondence is observed. Assuming an elongated shape along the [110] axis for the dot, a lateral extent of 40–50 nm is estimated from the energy distribution of excited-state resonances. The multitude of the PLE resonances may partly be due to the low symmetry of the dots which lifts the degeneracy of the states. They can be attributed to the excited energy-level structure of the dot exciton. Such one-to-one correspondence was also found by Brunner et al.[10] We assign these resonances to the excitation of the exciton because of the results of a PLE experiment under circularly polarized light excitation, which we will discuss later. The one-to-one correspondence in the PLE features, together with the intensity evolutions of X and XX as well as the overall agreement with theory, conclusively proves that they are emitted from
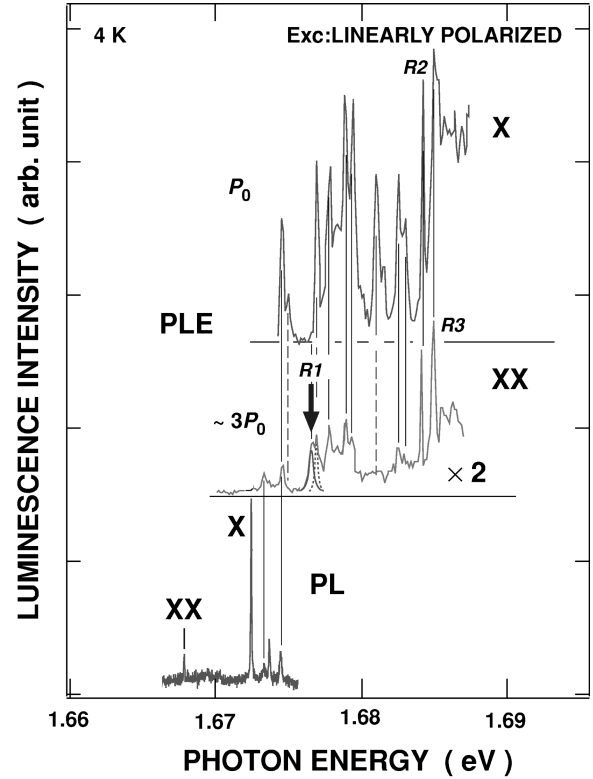
FIG. 5. Photoluminescence excitation spectra taken on exciton (X) and biexciton (XX) lines at 4 K under an excitation density ($\simeq 100$ W/cm^2). Excitation source is linearly polarized. Vertical bars indicate correspondence between resonances in X and XX. The line labeled $R1$ appears only in the XX-PLE spectrum.

the same In$_x$Ga$_{1-x}$As disk, and this supports the biexcitonic origin of the XX transition. The reason for this one-to-one correspondence will be discussed later.

PLE spectra were found to be extremely sensitive to excitation power density. PLE spectra show nonlinear behaviors when excitation density is increased. The spectra taken on X are in Fig. 6 for four different excitation densities—P_0, $2P_0$, $2.8P_0$, and $4P_0$—where P_0 is about 200 W/cm^2. When the excitation density is increased, the PLE spectrum changes nonlinearly: Some resonant features first grow almost linearly and then decrease, and this is accompanied by noticeable resonance line broadening. The broadening seems to be accompanied by the growing absorption between discrete resonances, which may be due to the increase of the overlapping contributions of a number of absorption resonances with small oscillator strength. Most remarkably, when the excitation density is increased further, the resonances labeled $R2$ and $R3$, which have large oscillator strength, turn into ''dips.'' These behaviors can be attributed to the nonlinear population of exciton states according to Eqs (1a)–(1c): Under high excitation density, the biexciton state population is substantial, therefore there should be a drop in the relative exciton state population as Fig. 4 shows. As a result of the saturation of the exciton state, the exciton absorption is bleached at the ground state as well as at the excited states. At highest excitation ($4P_0$), we also found the emergence of a new resonance $R1$. Such resonances only emerge when the exciton population is nearly saturated and they can be attributed to the transitions creating another exciton into a dot.
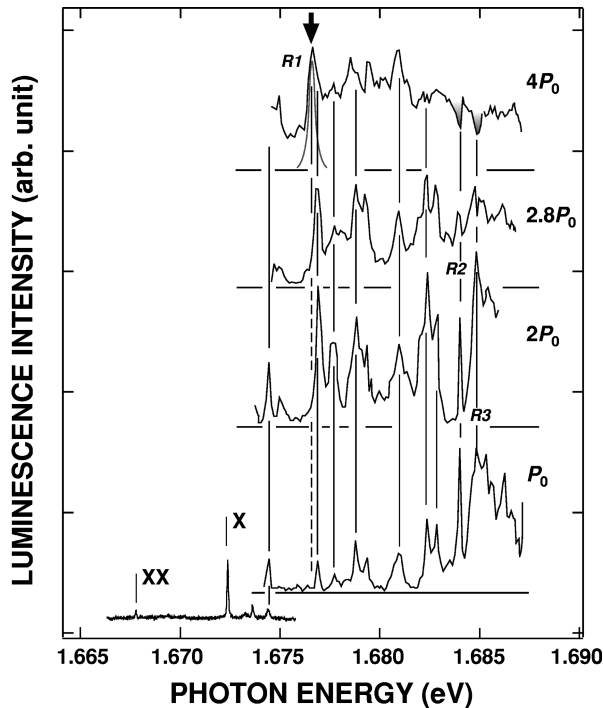
FIG. 6. PLE spectra taken on an exciton (X) line under a variety of excitation power densities, P_0, $2P_0$, $2.8P_0$, and $4P_0$, where P_0 is about 200 W/cm^2. Under the highest excitation density, excited state resonances labeled $R2$ and $R3$, which seem to have very large oscillator strength, appear as a ''dip.'' Also an emergence of a new resonance labeled $R1$ can be observed.

FIG. 7. PLE spectra of exciton and biexciton lines taken under linearly polarized excitation (a), and those under circularly polarized excitation (b). For (b), excitation is σ^+ and PL is σ^+. In the XX PLE spectrum, the $R1$ transition is visible.

A similar PLE experiment was done on both the X and XX lines but with circularly polarized excitation. The PL of either left- or right-handed helicity (σ^+ and σ^-) with the axis along the direction of light propagation was analyzed under an excitation of one of the two helicities. Figure 7(b) shows the PLE spectra for σ^+ excitation and σ^+ detection. For X, almost all the PLE resonances observed under linearly polarized excitation can also be observed under circularly polarized excitation. In distinct contrast, most of the PLE features of XX observed under the excitation of linear polarization [Fig. 7(a)] disappear or emerge only weakly, except for two or three higher-lying peaks labeled $R2$ and $R3$. Therefore, the observed exciton PLE resonances are due to the excited exciton states as discussed before. The $R1$ line observed under linear excitation cannot be seen. A straightforward conclusion is that circular polarization only excites an exciton with one of two spin orientations and therefore it cannot create an exciton with the other spin orientation and either a biexciton composed of two excitons with opposite spins. The same argument is applied to the disappearance of the $R1$ transition; because successive two-step transitions, each of which creates the same spin exciton into the dot, cannot populate a biexciton. The higher-lying biexciton PLE resonances, $R2$ and $R3$, which remain under circular excitation and are also observed in the exciton PLE spectrum, can be the optical transition allowed even under the circular polarized light of one of the two helicities. In a recent theory of exciton/biexciton optical processes of semiconductor quantum dots,[25] a two-photon transition directly creates a biexci-

ton with an angular momentum $J=2$ that is expected to be allowed. We therefore assign $R2$ and $R3$ to be such transitions.
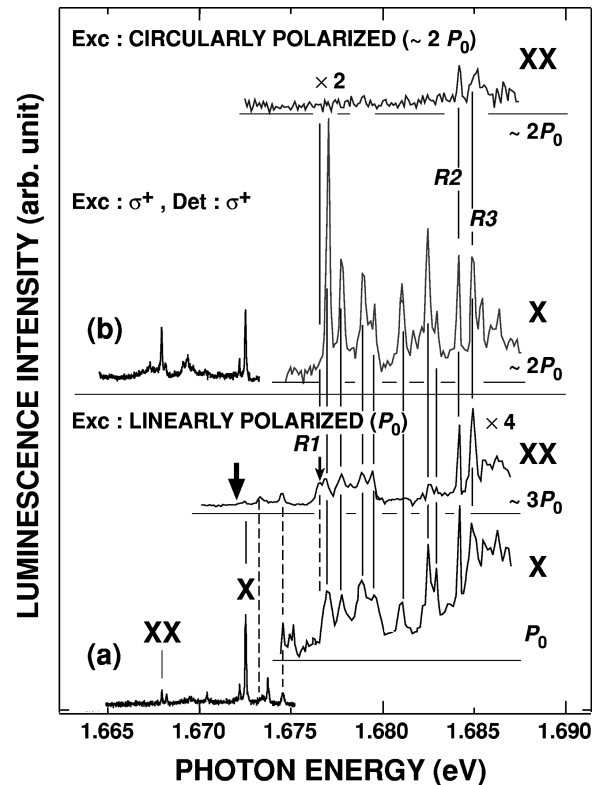
One may notice also that the PLE resonances are much more clearly resolved under circular excitation than those recorded under linearly polarized excitation. This may be due to the absence of the broad and densely distributed spectral contribution of the biexciton. Circular excitation will eliminate the biexcitonic contribution in the absorption spectrum leaving only exciton creation processes except for the two-photon transitions discussed above. Inferred broadened biexciton resonances can be explained by their higher energies and shorter dephasing time.

C. Symmetry properties

At this point, it is useful to review some details on the symmetry of the electron and hole Bloch functions and that of the excitons. The conduction-band s states and the valence-band p states are represented in the cubic zincblende T_d group as $^1\Gamma_1$ and $^3\Gamma_5$, respectively. In the double group representation, the $^1\Gamma_1$ conduction band becomes $^2\Gamma_6$ and the $^3\Gamma_5$ transforms to $^2\Gamma_7 \oplus {}^4\Gamma_8$. Spin-orbit coupling lifts the latter degeneracy and splits off the $^2\Gamma_7$ band, leaving the $^4\Gamma_8$ as the ground state of the holes. In a quantum well, which lowers the T_d symmetry to D_{2d}, $^4\Gamma_8$ bands split further into $^2\Gamma_6$ (light hole) and $^2\Gamma_7$ (heavy hole) bands. Of these, we are interested in the latter because they form the uppermost valence bands under quantum-well confinement. Excitons formed from the $^2\Gamma_6$ conduction-band electron and

$^2\Gamma_7$ valence-band hole have symmetry $^2\Gamma_6\otimes{}^2\Gamma_7={}^2\Gamma_5$ $\oplus{}^1\Gamma_3\oplus{}^1\Gamma_4$, i.e., a doubly degenerate $^2\Gamma_5$ exciton with (x,y) symmetry and two nondegenerate dark exciton states. The $^2\Gamma_5$ exciton states directly couple to light propagating perpendicular to the well, with an in-plane polarization along either x or y, acting as a state with total Bloch function angular momentum $I=1$. The $^1\Gamma_3$ exciton transforms like x^2-y^2, while the $^1\Gamma_4$ exciton transforms like xy. It is the $I=1(I_z=\pm1)$ exciton state ($^2\Gamma_5$) that is optically excited. As all the optically excited states have a zero angular momentum (L) for the envelope function, I also equals the total angular momentum for such states. From these exciton states, we may generate biexciton states: In the D_{2d} group representation, we have

$$^2\Gamma_5\otimes{}^2\Gamma_5={}^1\Gamma_1\oplus{}^1\Gamma_2\oplus{}^1\Gamma_3\oplus{}^1\Gamma_4,$$

$$^2\Gamma_5\otimes{}^1\Gamma_3={}^2\Gamma_5,$$

$$^2\Gamma_5\otimes{}^1\Gamma_4={}^2\Gamma_5,$$

$$^1\Gamma_3\otimes{}^1\Gamma_3={}^1\Gamma_1,$$

$$^1\Gamma_4\otimes{}^1\Gamma_4={}^1\Gamma_1,$$

$$^1\Gamma_3\otimes{}^1\Gamma_4={}^1\Gamma_2.$$

Biexciton states with the Bloch function angular momentum $J=0$, 1, or 2 are formed. Of these states, the $^2\Gamma_5\otimes{}^1\Gamma_3$ state and $^2\Gamma_5\otimes{}^1\Gamma_4$ state of a biexciton may act as $J=1$ states and are optically allowed. Therefore, either the product made up with two $^1\Gamma_3$ excitons or that with two $^1\Gamma_4$ excitons may be the ground state of biexciton as $J=0$ because they are symmetric under exciton exchange. The $^2\Gamma_5\otimes{}^2\Gamma_5$ biexciton state is made up with the exciton pair of $I=1$ and may act as a $J=2$ state. It is allowed for two-photon absorption because the two-photon operator has the same symmetry. In the notations above, we distinguish the total Bloch function angular momenta of excitons and biexcitons as I and J, respectively, using the notations adopted by Nair and Takagahara.[25] An important implication of the theory of exciton/biexciton transitions in spherical CuCl quantum dots is that the excitation of the weakly correlated exciton-pair states dominates the excited-state absorption. Although the present system is of lower symmetry than D_{2d} and the spin combination is much more complicated, a similar exciton-biexciton transition will be observed.

D. Modeling of exciton/biexciton transitions

The observed biexciton transitions are summarized in Fig. 8. Only allowed transitions are presented for circular polarizations.

The transition scheme that corresponds to the PLE transition $R1$ is described as (a). It involves the absorption from the $I=1$ exciton states to the biexciton state. Here, the absorption to create an $I=1$ exciton is allowed whatever the optical orientation is. Once the radiative exciton state, which is of $I=1$, is filled following the relaxation, the subsequent absorption of a photon creates the biexciton of $J=0$, 1, or 2. However, because of the biexcitonic nature, the optical orientation of the first and the second photons should be oppo-
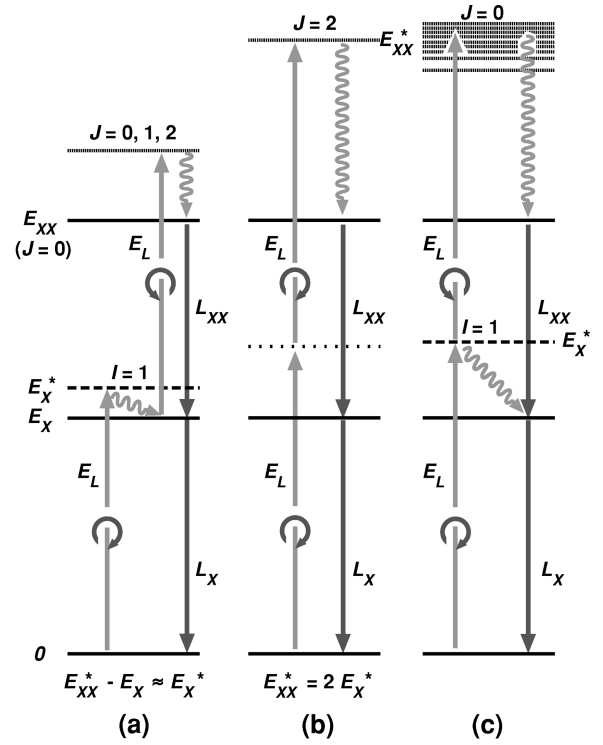
FIG. 8. Schematic representations of the observed excited state absorption resonances of exciton and biexciton. $R1$ is identified as absorption to create the first exciton followed by energy relaxation and subsequent absorption from the exciton ground state ($I=1$) into the biexciton excited state, (a). First and second transitions are allowed for two photons of opposite optical orientations. Two-photon absorption directly into the $J=2$ biexciton excited state (b) for observed transions $R2$ and $R3$. Two photons are of the same optical orientations. The other transitions observed in PLE spectra are classified as scheme (c). A two-step absorption process, first photoabsorption into the $I=1$ exciton excited state and simultaneous absorption into the biexciton excited state, creates biexciton. It is allowed for a photon pair with opposite optical orientations

site. The biexciton is formed only when the excitation permits the exciton population of both spin orientations; the process is forbidden for circular polarization. $R1$ (in Figs. 5 and 6) is observed in the exciton excitation spectrum as well as in the biexciton excitation spectrum when excitation photons are linearly polarized and the exciton state is nearly saturated. It vanishes completely under circularly polarized excitation. These features are all well interpreted within the scheme (a). Therefore, we assigned $R1$ as the absorption from the $I=1$ exciton states to the biexciton state.

The two-photon absorption to the $J=2$ biexciton state is described as (b). We assign two higher-lying PLE features, $R2$ and $R3$, to two-photon transitions which directly create $J=2$ biexciton states. The two-photon transition is allowed for linearly and circularly polarized photons. Evidently, $R2$ and $R3$ satisfies this. We conclude also that this two-photon absorption creates directly the weakly correlated exciton pair state.[15] The weakly correlated exciton pair state of $J=2$ in a large dot is well described by a product of two independent exciton wave functions and thus has an oscillator strength almost twice as large as that of the exciton state. It may therefore have an outstanding strength like $R2$ and $R3$.

The other PLE resonances observed are classified into the scheme in Fig. 6(c). Here, the absorption of a photon of a given optical orientation (denoted as E_L) creates an exciton of $I=1$ with a corresponding spin. The subsequent photon absorption from the excited $I=1$ exciton state to the biexciton is, however, allowed only for a photon with the opposite optical orientation. At a low excitation density, the first photon absorption is dominant. For higher excitations at which the exciton state saturates, the second absorption is prevailing over the first process. The net absorption for the biexciton creation is proportional to the product of the energy-level density distribution of excitons and that of biexcitons. Because the energy-level density distribution of the biexciton as a product of two excitons is much higher, the net absorption is determined by the sparse distribution of exciton levels. Accordingly, the biexciton PLE features resemble the exciton PLE features: it is the origin of the one-to-one correspondence between exciton and biexciton PLE features. With the excitation of circular polarized light, the second absorption to the biexciton is forbidden unless the partial spin-flip is allowed; that is what we observed.

In all cases, (a) through (c), both the exciton and biexciton luminescence can be observed, respectively, as L_X and L_{XX}. Although the details of the biexciton creation are not fully understood at this stage, the present experimental results strongly suggest these three schemes as dominating optical processes in the quantum-dot exciton/biexciton system.

Having discussed the origin of the observed excited-state transitions of the exciton and biexciton, we now analyze several important points from the preceding paragraph. It is interesting again to point out the absence of $R1$ resonance under spin-selective excitation. This implies that a resonantly excited exciton with a given optical-spin orientation never flips into the other orientation even during the energy relaxation followed by thermalization before radiative recombination. In other words, if spin relaxation occurs before radiative recombination, we may observe biexciton luminescence because two excitons with the same quantum number and energy but differing in spin orientation can coexist with finite probabilities within the time interval of the order of the biexciton recombination lifetime. The vanishingly small biexciton PL signal at most of the exciton excited state resonances shown in Fig. 7(b) can then also be understood as a result of the suppression of spin relaxation in the present quantum disk system. The full quantization of the quantum-well energy spectrum into 0D by additional lateral confinement makes all the elastic processes inefficient that have usually been invoked to explain the rapid relaxation of spin in bulk materials[32–35] or in 2D systems.[36] As the density of states between discrete levels is zero, the relaxation of photogenerated excitons between levels with different spins can only take place by a change in energy and magnetic moment. No elastic process to flip the electron spin can occur because there is no state available between levels due to the absence of energy versus momentum dispersion in all directions. The inhibition of the elastic spin-flip processes may thus lead to a substantial increase in the spin-relaxation time.[37,38] The present results strongly suggest the slowing down of spin relaxation. Our recent time evolution measurement on polarization-resolved photoluminescence also revealed that the spin relaxation time at 4 K is about twice as long as the

radiative recombination lifetime (400–500 ps).[29] Let us end the discussion by noting that spin relaxation in quantum dots may play a crucial role in the creation of biexcitons. This opens up a new aspect in quantum-dot physics that remains to be worked out. Work is now underway to unveil the role of spin-relaxation in quantum dots.

IV. CONCLUSIONS

In conclusion, we showed that biexciton optical response plays a crucial role in the optical process of the quantum dot. The biexciton effect was confirmed for most of the individual dots we examined: Not only exciton luminescence but also biexciton luminescence from the individual dots were observed in $In_xGa_{1-x}As$ self-organized structure, which manifested an enhancement of the biexciton effect in the mesoscopic quantum dot, which itself exhibited a biexciton binding energy more than 5 meV, much larger than in the quantum well or the bulk. Because of the enhanced biexciton, the excitation of an exciton occurs not only via its own excited states but also via its higher-lying excited biexciton states. Polarization dependent photoluminescence excitation is shown to be valuable to assign excited-state transitions to those via an exciton excited state or a biexciton excited state. By a detailed comparison of the exciton as well as biexciton excitation spectra, taken under spin-nonselective excitation (linear polarization excitation) and spin-selective excitation (circular polarization excitation), we managed to distinguish the exciton and biexciton excited states.

Most of the observed transitions were related to the exciton excited states. Some excitation resonances are assigned to the absorptions from the exciton ground states to excited biexciton states. We also found a candidate for the two-photon absorption which allows direct creation of biexcitons in the higher-lying excited state. Such biexciton states are considered to be a weakly correlated pair of excitons, which can have outstanding oscillator strength. Together with the recent results on CuCl nanocrystallites, weakly correlated exciton-pair states seem to have a quite general nature in 0D systems in the weak confinement regime and they may exist in other systems.

Finally, we note that as a consequence of the discrete nature of the spin-split levels, i.e., the zero density of states between the levels, there appears to be a strong tendency for the conservation of the electron magnetic moment which prohibits the creation of excitons with opposite spin. This opens up a new experimental field in quantum dot physics regarding the general understanding of exciton relaxation in 0D. We hope that our results may contribute to a better understanding of the spin-dependent properties of 0D systems.

[1] Y. Arakawa and H. Sakaki, Appl. Phys. Lett. **40**, 939 (1982).

[2] D. Leonard, M. Krishnamurthy, C. M. Reaves, S. P. Denbaars, and P. M. Petroff, Appl. Phys. Lett. **63**, 3203 (1993).

[3] D. Leonard, M. Krishnamurthy, S. Fafard, J. L. Merz, and P. M. Petroff, J. Vac. Sci. Technol. B **12**, 1063 (1994).

[4] R. Nötzel, J. Temmyo, and T. Tamamura, Jpn. J. Appl. Phys., Part 2 **33**, L275 (1994).

[5] H. Gotoh, H. Ando, and T. Takagahara, J. Appl. Phys. **81**, 1785 (1997).

[6] J.-Y. Marzin, J.-M. Gerard, A. Izrael, D. Barrier, and G. Bastard, Phys. Rev. Lett. **73**, 716 (1994).

[7] D. Gammon, E. S. Snow, B. V. Shanabrook, D. S. Katzer, and D. Park, Phys. Rev. Lett. **76**, 3005 (1996).

[8] S. Fafard, R. Leon, D. Leonard, J. L. Merz, and P. M. Petroff, Phys. Rev. B **52**, 5752 (1995).

[9] M. Grundmann, J. Christen, N. N. Ledentsov, J. Bohrer, D. Bimberg, S. S. Ruvimov, P. Werner, U. Richter, U. Gosele, J. Heydenreich, V. M. Ustinov, A. Yu. Egorov, A. E. Zhukov, P. S. Kop'ev, and Zh. I. Alferov, Phys. Rev. Lett. **74**, 4043 (1995).

[10] K. Brunner, G. Abstreiter, G. Bohm, G. Trankle, and G. Weimann, Phys. Rev. Lett. **73**, 1138 (1994).

[11] H. Kamada, J. Temmyo, M. Notomi, T. Furuta, and T. Tamamura, Jpn. J. Appl. Phys., Part 1 **36**, 4194 (1997).

[12] M. Notomi, T. Furuta, H. Kamada, J. Temmyo, and T. Tamamura, Phys. Rev. B **53**, 15 743 (1996).

[13] A. Forchel, R. Steffen, T. Koch, M. Mitchel, M. Albrecht and T. L. Reiecke, Semicond. Sci. Technol. **11**, 1529 (1996).

[14] E. Dekel, D. Gershoni, E. Ehrenfreund, D Spektor, J. M. Garcia, and P. M. Petroff, Phys. Rev. Lett. **80**, 4991 (1998).

[15] Y. Z. Hu, S. W. Koch, M. Lindberg, N. Peyghambarian, E. L. Pollack, and F. F. Abraham, Phys. Rev. Lett. **64**, 1805 (1990).

[16] Y. Z. Hu, M. Lindberg, and S. W. Koch, Phys. Rev. B **42**, 1713 (1990).

[17] M. Ikezawa and Y. Masumoto, Jpn. J. Appl. Phys., Part 1 **36**, 4191 (1997).

[18] H. Kamada, J. Temmyo, M. Notomi, T. Furuta, and T. Tamamura, *Extended Abstracts: 1996 International Conference on Solid State Devices and Materials* (Business Center for Academic Societies).

[19] R. Nötzel, J. Temmyo, and T. Tamamura, Nature (London) **369**, 131 (1994).

[20] R. Nötzel, J. Temmyo, H. Kamada, T. Furuta, and T. Tamamura, Appl. Phys. Lett. **65**, 457 (1996).

[21] M. Sugawara, Phys. Rev. B **51**, 10 743 (1995).

[22] V. Halonen, T. Chakraborty, and P. Pietilainen, Phys. Rev. B **45**, 5980 (1992).

[23] B. Adolph, S. Glutsch, and F. Bechstedt, Phys. Rev. B **48**, 15 077 (1993).

[24] U. Bockelmann, Phys. Rev. B **50**, 17 271 (1994).

[25] S. V. Nair and T. Takagahara, Phys. Rev. B **55**, 5153 (1997).

[26] Y. Z. Hu *et al.*, Phys. Rev. Lett. **64**, 1805 (1990).

[27] R. C. Miller, D. A. Kleinman, A. C. Gossard, and O. Munteanu, Phys. Rev. B **25**, 6545 (1982).

[28] G. W. 't Hooft, W. A. J. A. v. d. Poel, L. W. Molenkamp, and C. T. Foxon, Phys. Rev. B **35**, 8281 (1987).

[29] H. Gotoh, H. Kamada, H. Ando, and J. Temmyo, Appl. Phys. Lett. **72**, 1341 (1998).

[30] T. Takagahara, Phys. Rev. B **39**, 10 206 (1989).

[31] T. Takagahara, Phys. Rev. B **47**, 4569 (1993).

[32] *Optical Orientation*, edited by P. Meier and B. P. Zakharchcnya, Modern Problems in Condensed Matter Sciences Vol. 8 (North-Holland, Amsterdam, 1984).

[33] K. Zerrouatti, F. Fabre, G. Bacquct, J. Frandon, G. Lampel, and D. Paget, Phys. Rev. B **37**, 1334 (1988).

[34] G. Fishman and G. Lampel, Phys. Rev. B **16**, 820 (1977).

[35] M. I. D'yakonov and V. I. Perel', Zh. Eksp. Teor. Fiz. **60**, 1954 (1971) [Sov. Phys. JETP **33**, 1053 (1971)].

[36] C. Weisbuch, R. C. Miller, R. Dingle, A. C. Gossard, and W. Wiegmann, Solid State Commun. **37**, 219 (1981).

[37] M. Potemski, J. C. Maan, A. Fasolino, F. Ancilotto, K, Ploog, and G. Weimann, in *Proceedings of the Nineteenth International Conference on the Physics of Semiconductors, Warsaw, 1988*, edited by W. Zawadzki (Polish Academy of Sciences, Warsaw, 1989), p. 235.

[38] W. Heller and U. Bockelmann, Phys. Rev. B **55**, R4871 (1997).